Investigations of nanoscale helical pitch in smectic-C^*_α and smectic-C^* phases of a chiral smectic liquid crystal using differential optical reflectivity measurements

V. P. Panov,[1] B. K. McCoy,[2] Z. Q. Liu,[2] J. K. Vij,[1,*] J. W. Goodby,[3] and C. C. Huang[2]
[1]*Department of Electronic and Electrical Engineering, Trinity College, University of Dublin, Dublin 2, Ireland*
[2]*School of Physics and Astronomy, University of Minnesota, Minneapolis, Minnesota 55455, USA*
[3]*Department of Chemistry, University of York, York, YO10 5DD, United Kingdom*
(Received 10 February 2006; revised manuscript received 16 May 2006; published 6 July 2006)

Differential optical reflectivity (DOR) was used to study the temperature dependence of the short helical pitch in freestanding films of a liquid crystal compound. The experimentally measured DOR signal was fitted using Berreman's 4×4 matrix method to get the pitch value in the smectic-C^*_α (SmC^*_α) phase. The results show continuous evolution of the pitch between the smectic-C^* and SmC^*_α phases. In SmC^*_α, the pitch decreases as temperature increases and is found to level off at 16 ± 1 smectic layers at the SmC^*_α to smectic-A^* transition.

DOI: 10.1103/PhysRevE.74.011701 PACS number(s): 61.30.Gd, 64.70.Md, 77.84.Nh, 83.80.Xz

I. INTRODUCTION

The properties of chiral liquid crystalline phases between smectic-A^* (SmA^*) and antiferroelectric smectic-C_A (SmC^*_A) have recently attracted special attention due to their potential applications to various electro-optical switching devices. They offer significant scientific challenge to condensed matter physicists for understanding the physical basis of the emergence of the novel subphase structure that arises in these materials. Antiferroelectricity was suggested to arise in chiral doped liquid crystals by Beresnev *et al.* [1] using the pyroelectric technique; however, detailed investigations did not begin until Chandani *et al.* [2] confirmed it through a series of experiments in a prototype single chiral compound MHPOBC. The phase sequence is generally as follows, with increasing temperature: SmC^*_A, intermediate SmC^*_{FI1} (three-layer unit cell) [2,3] and SmC^*_{FI2} (four-layer unit cell) [4,5], SmC^* [6], SmC^*_α [2,7], and SmA^*. The layer structure in the various phases was directly confirmed for the first time by resonant x-ray scattering by Mach *et al.* [8], where the two ferrielectric phases with three- and four-layer structures were named Ferri 1 and Ferri 2, respectively. On the other hand, the rich variety of phases that were initially noticed through a careful differential scanning calorimetry (DSC) in MHPOBC [9] has initiated the development of new theoretical approaches for description of these phase transitions [10–14]. In the liquid crystalline phases mentioned above, apart from SmA^*, chiral molecules are spontaneously tilted at an angle θ with respect to the layer normal. Among them the SmC^*_α phase has attracted special attention due to seemingly apparent contradiction between its observed optical uniaxiality and its nonzero tilt angle [7,15–17]. In SmC^* and SmC^*_α, the azimuthal direction of the molecular tilt changes by a constant angle for any two adjacent layers; the tilt direction forms a helical structure. The pitch of this helix is of the order of the wavelength of visible light for SmC^*, while SmC^*_α is characterized by an incommensurate nanoscale helical pitch [8,16–22].

Figure 1 represents the temperature dependence of the selective reflection wavelength in (*R*)-1-methylheptyl 4-(4′-*n*-dodecyloxybiphenyl-4-yl-carbonyloxy)-3-fluorobenzoate, (*R*)-12OF1M7 [23]. The data were obtained in oblique transmission geometry with an angle of incidence of 20°. In this case we can easily distinguish between SmC^*_A and SmC^* phases, since SmC^* possesses the full-pitch selective reflection band (II), while the half-pitch band (I) can be observed in both phases. Between them the helical pitch diverges to values well above the visible wavelength range, indicating the presence of the intermediate phases, SmC^*_{FI2} and SmC^*_{FI1} [24], which can be identified using additional measurements [23–27]. One can see that the helical pitch in SmC^* decreases steeply near 90 °C. The shortest pitch measured by the selective reflection apparatus using the full-pitch band is less than 30 smectic layers (i.e., about 100 nm, which corresponds to the full-pitch selective reflection wavelength of 350 nm). However, smaller values of the helical pitch are not accessible for investigation by selective reflection since the material is opaque in the UV region. Meanwhile the presence of the short-pitch SmC^*_α phase in 12OF1M7 was confirmed by dielectric, pyroelecric [28], and circular dichroism [29]

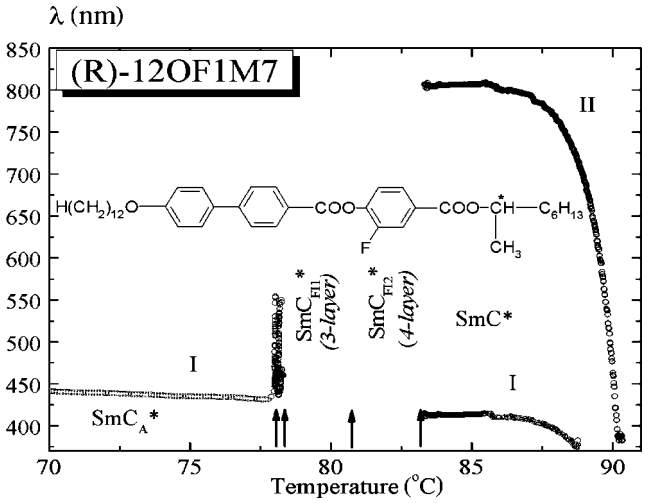

FIG. 1. Characteristic reflection peaks for 20° oblique incidence in a 60 μm thick, freestanding film of (*R*)-12OF1M7.

*Author to whom correspondence should be addressed. Electronic address: jvij@tcd.ie

measurements. SmC^*_α also has been observed in preliminary differential optical reflectivity (DOR) measurements [27]. In this paper we investigate the behavior of the helical pitch in the SmC^*_α phase of (*S*)-12OF1M7, which is proven to possess the same phase sequence as the (*R*) enantiomer. Our DOR data provide the following phase transition temperatures under heating: SmC^*_A (78.4 °C) SmC^*_{FI1} (81.1 °C) SmC^*_{FI2} (84 °C) SmC^* (91.4 °C) SmC^*_α (92.4 °C) SmA^*. In contrast to the selective reflection technique, DOR is not limited by the UV absorption of the liquid crystal, since it is not based on measurements at the corresponding wavelength but on observation of the change in the birefringence of a freestanding film as a function of temperature.

The short helical pitch in SmC^*_α makes this phase nearly uniaxial when observed in bulk samples using visible light. The birefringence of the film is determined by any incomplete turns of the helix in it which may occur at the surfaces of the sample. In addition, as shown by null transmission ellipsometry [30,31], the surface layers have a significant tilt even in the SmA^* phase; in SmC^*_α the molecules are tilted additionally from the layer normal in the surface layers, forming more ordered molecular arrangements than in the bulk. Therefore, the surfaces make a major contribution to the total film birefringence, acting as a pair of birefringent plates near the two outer surfaces attached to the rest of the film. Having no restriction from the outside (liquid crystal-gas interface), the surface layer tilt orientation follows the tilt orientation of the adjacent bulk layer. Upon changing the helical pitch in a film with a fixed number of layers, the tilt orientations of the two surfaces mutually rotate, causing periodic oscillations in the birefringence of the entire film. Because the film is birefringent, the reflectivity of the film is different for different polarizations of incident light. DOR measures reflectivity for light polarized parallel and perpendicular to the plane of incidence. By measuring the *difference* between nearly equal intensities of the two orthogonal polarizations we can easily resolve the oscillations in the birefringence of the film. In this paper, the helical pitch in SmC^*_α as a function of temperature is extracted from DOR data by simulating the DOR signal using an appropriate model. The pitch is confirmed to be consistent with measurements from other methods at the high and low temperature ends of the SmC^*_α phase window. Nearest-neighbor and next-nearest-neighbor interaction strengths in a simple free energy expansion are derived from the pitch as a function of temperature.

II. EXPERIMENT

A detailed description of the differential optical reflectivity setup (Fig. 2) is given in Ref. [32]. A film thickness measurement procedure allowing a resolution of ±1 smectic layers for freestanding films with thicknesses of up to 100 layers is also given in [32].

The refractive indices and the smectic layer thickness in the SmA^* phase were determined by null transmission ellipsometry [30,31].

The freestanding films were prepared in a two-stage oven with a temperature resolution of 10 mK. The oven contained

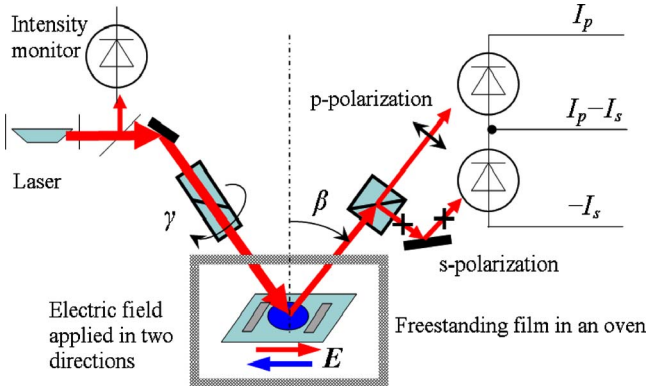

FIG. 2. (Color online) A schematic of the differential optical reflectivity system. Incident 632.8 nm HeNe laser light is polarized by a Glan-Thompson polarizer mounted on a rotatable stage. After being reflected off the film under investigation, the light is divided by a polarizing beam splitter into *p* and *s* polarizations, where *p* and *s* denote polarizations parallel and perpendicular to the incident plane, respectively. The signals acquired by two photodiodes are the difference, $I_p - I_s$, and the sum, $I_p + I_s$, of the intensities. The experiment is begun with the film in the SmA^* phase. The polarizer is rotated by the angle γ to yield $I_p - I_s = 0$, which allows the best use of the amplifier's dynamic range and facilitates the resolution of tiny changes of the optical properties of the film.

a 0.7 atm helium exchange gas. The films were drawn across a 9 mm diameter circular hole in a glass coverslip (150 μm thick) with two electrodes on opposite sides of the opening, allowing the application of an electric field in the plane of the film. The data were acquired during heating and cooling temperature ramps of 20–50 mK/min under an applied electric field of approximately ±5 V/cm parallel to the projection of the wave vector of the incident light on the plane of the film. The electric field applied is three orders of magnitude less than necessary for ferroelectric liquid crystal switching in device geometry; moreover, changing the field to 2.5 V/cm does not produce any visible difference in the data obtained. The field is too small to disturb the molecular arrangements in the liquid crystalline phase; however, it is large enough to stabilize a monodomain sample and align the net polarization of the structure along the field direction.

III. SIMULATIONS

The 4×4 matrix method [33] was used to simulate the reflectivity. Each smectic layer is modeled as a uniaxial slab with extraordinary index of refraction n_e along the long molecular axis and ordinary refractive index n_o along the other two principal molecular axes. Three parameters, layer thickness d (in the SmA^* phase), n_o, and n_e, used in simulations were obtained from our null transmission ellipsometry measurements. For 12OF1M7 in SmA^* phase, $d = 3.66 \pm 0.05$ nm, $n_o = 1.496 \pm 0.003$, and $n_e = 1.658 \pm 0.003$.

The temperature variation of the incommensurate nanoscale helical pitch (INHP) was found by simulating the data until the simulated $I_p - I_s$ values yielded the best match to the measured values. In particular, the positions of the extrema of the $I_p - I_s$ signal strongly depend on the temperature varia-

tion of the pitch. The amplitude of the oscillations is determined by the film reflectivity, and the biaxiality of the structure is associated with the bulk and surface tilt. The relatively small continuous change in this amplitude for a given film demonstrates small gradual change in the effective thickness of the surface layers [34]; thus, the fits were made without varying the number of surface layers with temperature. The tilt in the bulk as a function of temperature was found in a separate experiment [29]. The surface tilt was assumed to be constant with temperature, and its value was selected to provide the best fit to the $I_p - I_s$ data.

To simulate the reflectance, one needs to model the molecular arrangement in the film. In general, each smectic layer has its own tilt angle θ_j and azimuthal angle φ_j. Here the index j denotes the layer number. For simplicity we assume an integral number N_S of surface layers with a fixed surface tilt angle θ_S on each surface and a uniform tilt angle θ in the bulk taken from a separate experiment on thick, freestanding films [24,29,35]. The azimuthal angle for surface layers was considered to be either constant (ferroelectric) or changing by π from layer to layer (antiferroelectric). While more complicated surface structures may exist in the real system, this simple approximation properly reflects the nature of the surface layers studied in detail before [27,31]. In the bulk, the azimuthal angle changes linearly from layer to layer, forming a helical pitch P. Therefore the tilt and azimuthal angles for a film with ferroelectric surface layers are

$$\theta_j = \begin{cases} \theta_S, & 1 \leqslant j \leqslant N_S \\ \theta, & N_S < j < N - N_S \\ \theta_S, & N - N_S \leqslant j \leqslant N, \end{cases}$$

$$\varphi_j = \begin{cases} \varphi_0, & 1 \leqslant j \leqslant N_S \\ \varphi_{j-1} \pm \dfrac{2\pi d \cos\theta}{P}, & N_S < j \leqslant N - N_S \\ \varphi_{j-1}, & N - N_S < j \leqslant N, \end{cases} \tag{1}$$

or

$$\varphi_j = \begin{cases} \varphi_0, & j = 1 \\ \varphi_{j-1} + \pi, & 1 < j \leqslant N_S \\ \varphi_{j-1} \pm \dfrac{2\pi d \cos\theta}{P}, & N_S < j \leqslant N - N_S \\ \varphi_{j-1} + \pi, & N - N_S < j \leqslant N \end{cases} \tag{2}$$

for antiferroelectric surface layers, where N is the total number of layers in the film and the sign of the azimuthal angle increment is determined by the handedness of the helical pitch.

The angle φ_0 is determined by interaction of the net polarization of the film with the applied electric field. Each layer has a spontaneous polarization perpendicular to the tilt direction, due to symmetry breaking when the molecules are tilted. The polarization in each layer is approximately proportional to the tilt angle. The net polarization of the film is the sum of the vector polarizations of each layer. Therefore, the net polarization of the film can be characterized by

$$\varphi_{orient} = \arg\left(\sum_{j=1}^{N} \sin(\theta_j) \exp(i\varphi_j) \right). \tag{3}$$

The net film polarization is aligned along the external electric field, so we require either $\varphi_{orient}=0$ or $\varphi_{orient}=\pi$, depending on the sign of the applied electric field. In practice, φ_{orient} is calculated assuming $\varphi_0=0$, then the azimuthal angles in Eqs. (1) or (2) are recalculated using $\varphi_0=-\varphi_{orient}$ or $\varphi_0=\pi-\varphi_{orient}$.

Although in the real liquid crystal film the surface layers are much more complicated than described above and the surface layers play a critical role in the DOR signal, this simple model allows us to determine the INHP as a function of temperature with an accuracy better than 10%. This is because the positions of the extrema of the $I_p - I_s$ signal are much more sensitive to the variations of the pitch than to the other fitting parameters.

To begin the fitting process, the pitch in the SmC^* region was assumed to be equal to the pitch measured by selective reflection. The pitch measured by selective reflection at 90 °C was used as an initial guess for finding the temperature dependence of the pitch. Because the pitch decreases with increasing temperature, $I_p - I_s$ was calculated as a function of pitch for pitch values shorter than found at 90 °C. The pitch values that gave extrema of the $I_p - I_s$ simulation were assigned to the temperatures at which the corresponding extrema of $I_p - I_s$ occurred in the experiment. Interpolation between these points gave an initial approximation of the pitch vs temperature curve. Subsequent iterations produced the pitch vs temperature curve that best fits the experimental data, shown in Fig. 4.

Figure 3 presents an example of fitting the same experimental data from a 230-layer film using different surface layer structures. The circles and crosses denote the experimental data for the two opposite directions of the applied electric field, while the solid lines denote the simulation results. The simulations were obtained using two tilted layers per surface ($N_S=2$, $\theta_S=23°$). As shown earlier [36], the tilted surface layers can form either ferroelectric [Eq. (1)] or antiferroelectric [Eq. (2)] structures. The plot on the top of Fig. 3 presents the simulations using the set of equations (1) in comparison to the bottom plot, where the simulations were performed using the set of equations (2). The same pitch vs temperature curve was used for both plots. One notes that in both cases the extreme points of the $I_p - I_s$ simulations are in good agreement with the experimental data in spite of such a dramatic difference in the surface structures.

The temperature dependence of the helical pitch used for this simulation is given in Fig. 4 by circles. The simulation parameters are $N=230$ and incidence angle $\beta=13.7°$. The incidence polarization direction and beam intensity (arbitrary units) are $\gamma=40.1°$ and $I_0=42$ for the simulation using ferroelectric surface layers and $\gamma=40°$ and $I_0=43$ for antiferroelectric surface layers.

The helical pitch decreases down to 16 ± 1 smectic layers on heating. The obtained pitch length could vary slightly depending on the number of surface layers N_S used for simulations. This is easy to explain by the simplicity of our

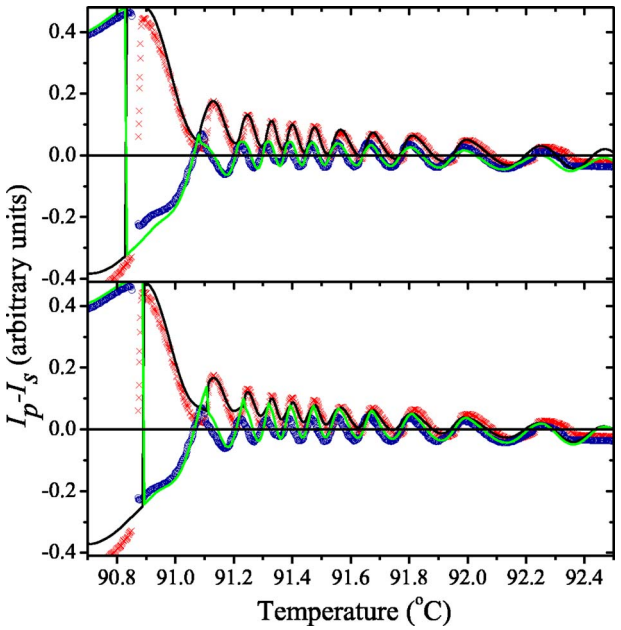

FIG. 3. (Color online) 4×4 matrix fitting of a 230-layer film using different surface structures. The solid lines represent simulation results and the symbols (red crosses and dark blue circles for the two opposite directions of the electric field) represent experimental data.

model. The helical structure present in the bulk is absent in the surface layers, so the effective length of the helical portion of the film is the thickness of the film minus $2N_S$ layers. A plot of the number of oscillations vs thickness of the film is linear. A linear fit using all films that we measured yielded an intercept of approximately 4–6 layers, meaning that there are 2–3 tilted layers at each surface. The real value of the pitch should be close to the results of the simulations with two layers per surface; similar values of the number of surface layers have been obtained by our null transmission ellipsometry experiments [31]. In Fig. 3, the film thickness

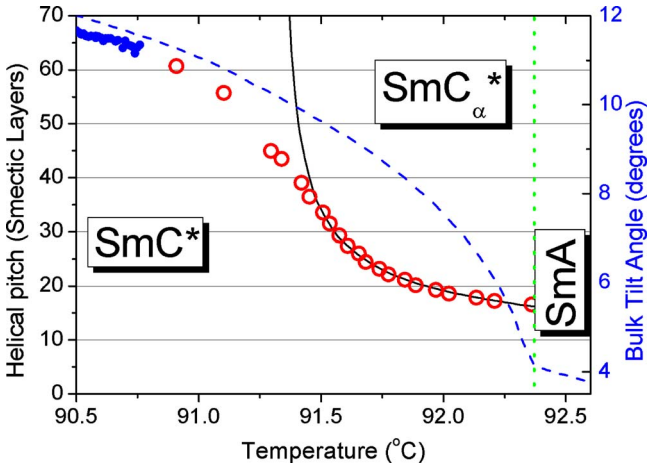

FIG. 4. (Color online) Temperature dependence of helical pitch (open circles) for a 230-layer film, fitted using the next-nearest-neighbor approximation (solid line). The pitch values obtained from selective reflection using the half-pitch band are shown by closed circles. The corresponding bulk tilt angle is shown by a dashed line.

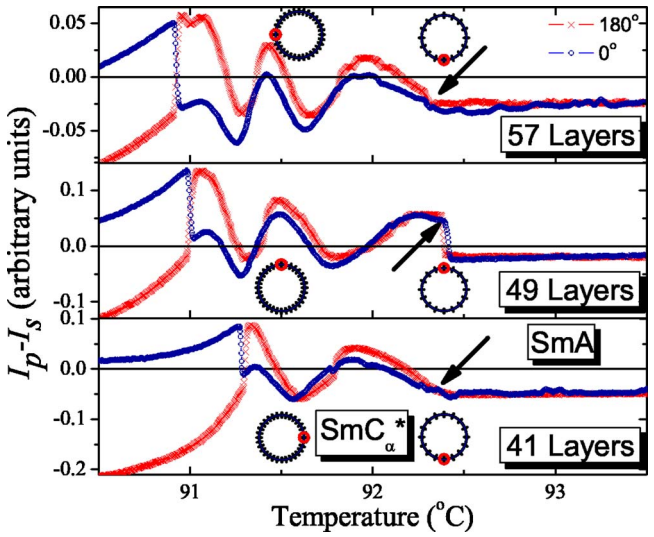

FIG. 5. (Color online) The phase of the oscillations of the DOR signal at the SmC^*_α-SmA^* transition varies periodically with film thickness. The periodicity is approximately 16 layers. Red crosses and dark blue circles denote the data obtained using two opposite field directions. The wheels illustrate the periodicity of the signal with film thickness.

was chosen to be much larger than the surface layer thickness in order to minimize uncertainty in the pitch due to the number of surface layers.

The periodicity of 16±1 smectic layers at the high temperature end of the SmC^*_α phase can be confirmed by comparing DOR results from a series of thin films with a single layer increment in thickness [34]. DOR measurements were performed on 21 films with thicknesses varying from 41 to 61 smectic layers. Choosing appropriate thicknesses is crucial because this method relies on the accurate determinations of the thickness of each film. We find thickness by measuring the reflectivity of the film for green and red laser light at several incident angles. The reflectivity oscillates with the film thickness with a period of about 20 layers. When the reflectivity is not near an extremum, we can determine the thickness of a single film to ±1 layer and the difference in thickness of two films precisely. The thickness measurements become ambiguous near extrema of the reflectivity. The 21 films studied were chosen so that the thickness could be accurately determined for every film in the series. In order to determine the helical pitch, the number of films studied must be larger than the number of layers in the helical pitch. Figure 5 presents examples of the $I_p - I_s$ signal for three films of selected thicknesses. The arrows indicate the SmC^*_α-SmA^* phase transition. We do not indicate the point of the SmC^*-SmC^*_α phase transition here since the transition is proven to be continuous. Note that the jumps of the optical signal at 91.3 °C (41 layers), 91.0 °C (49 layers), and 90.9 °C (57 layers) can possibly be confused with the SmC^*-SmC^*_α phase transition; however, these are just interchanges between the signals related to the two directions of the applied electric field at the points where the vector of the net polarization of the film passes its zero value. This is illustrated by Fig. 6, where the two simulated $I_p - I_s$ signals for a simple film are given as functions of the pitch together

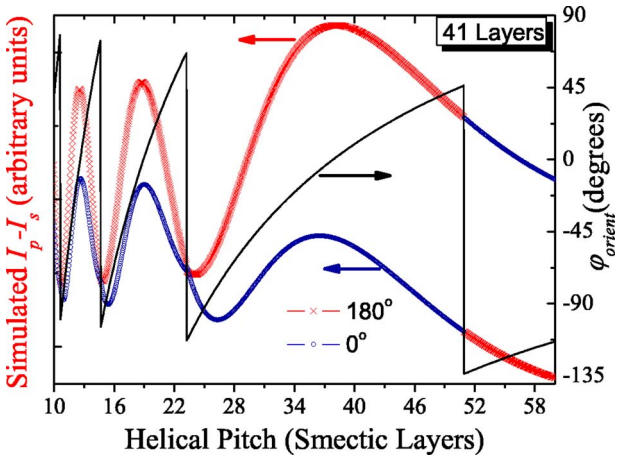

FIG. 6. (Color online) Simulated helical pitch dependencies of $I_p - I_s$ signals (red crosses and dark blue circles for the two opposite directions of the electric field) for a simple helical structure in an external field show abrupt interchanges of the signals similar to those found in the experiment. The corresponding behavior of the angle φ_{orient} obtained from Eq. (3) assuming $\varphi_0=0$ is given by the black solid line. The simulation parameters of the film with ferroelectric surface layers are: $N=41$, $N_S=2$, $\theta_S=23°$, $\theta=5°$.

with the angle φ_{orient} obtained from Eq. (3), assuming $\varphi_0=0$. Naturally, for different film thicknesses the interchanges happen at different temperatures, i.e., these jumps correspond to different values of the helical pitch. One clearly notes the periodicity of approximately 16 layers in the phase of the DOR signal oscillations at the SmC^*_α-SmA^* transition point, meaning that the helical pitch is approximately 16 layers. In a similar way one can find that at 91.5 °C the difference of 16 layers corresponds to approximately one half of the periodicity of the signal, which is in good agreement with the results obtained from the thicker films using the 4×4 matrix method (Fig. 4). This confirms the validity of our fitting procedure. Successful measurement of a 16-layer pitch represents a significant extension of our work beyond previous applications of this method.

IV. DISCUSSION

To analyze the evolution of the pitch found in the experiment, we employed the same free energy expansion as was used previously for the compounds 10 and 11-OHFBBB1M7 [37]. Expanding the free energy due to the interlayer interactions up to the next-nearest-neighbor term, one obtains

$$G = \frac{1}{2}\sum_{j=1}^{N}\left[a_1(\vec{\xi}_j \cdot \vec{\xi}_{j+1}) + a_2(\vec{\xi}_j \cdot \vec{\xi}_{j+2})\right] \tag{4}$$

where $\vec{\xi}_j = \theta_j(\cos\varphi_j, \sin\varphi_j)$ is the two-dimensional order parameter describing the magnitude θ_j and direction φ_j of the molecular tilt. Here we neglect the energy of the surface interactions, since the pitch evolution as a function of temperature was obtained from relatively thick (more than 200 layers) films. The coefficients a_1 and a_2 represent the strength of the nearest-neighbor and the next-nearest-neighbor interactions, respectively. The tilt angle in the SmC^*_α phase varies between approximately 4° and 11° over a 1 °C temperature range. In such a narrow temperature range the tilt angle can be approximated with reasonable accuracy by a simple formula, $\theta=A[(T_c-T)T_c]^{0.33}$ [38], derived from the extended mean field model. The fitting parameters obtained are $T_c=(92.44\pm0.02)$ °C and $A=69.3°\pm0.1°$. The tilt angle more than doubled over the SmC^*_α temperature region. We expand a_1 and a_2 to second order in θ as $a_1=-a+b\theta^2$ and $a_2=c+d\theta^2$, where a, b, c, and d are temperature independent quantities. This simple free energy expression yields a very good description of the temperature dependence of the INHP in the SmC^*_α temperature range. Beyond selecting the handedness of the INHP, no chiral terms are necessary.

By minimizing G, we find the approximate solution for the change in the azimuthal angle between adjacent layers to be

$$\delta\varphi = \arccos\left[\frac{1-\dfrac{b\theta^2}{a}}{4\left(\dfrac{c}{a}+\dfrac{d\theta^2}{a}\right)}\right]. \tag{5}$$

The pitch in terms of the number of smectic layers is $2\pi/\delta\varphi$. In Fig. 4 the fitted functions of the pitch are given by the solid line. The fitting yields $b/a=(18.2\pm0.1)$ rad^{-2}, $d/a=(-5.2\pm0.2)$ rad^{-2}, and $c/a=(0.27\pm0.01)$.

In the SmC^*_α phase $a_1<0$, indicating ferroelectric coupling of nearest-neighbor layers, and $a_2>0$, representing antiferroelectric coupling of next-nearest-neighbor layers. The absolute values of both a_1 and a_2 decrease on cooling to the SmC^* phase. This is similar to previously reported results for 11-OHFBBB1M7 [37]. The changes of the absolute values of a_1 and a_2 are slightly above 50% on cooling toward the SmC^* phase. The absolute value of a_1 exceeds the absolute value of a_2 by a factor of at least four. This is also reasonable since the interlayer interactions have to vanish quickly with distance to allow the free energy expansion to be truncated after the next-nearest-neighbor term.

V. CONCLUSIONS

Measuring the small difference in birefringence of freestanding films by differential optical reflectivity enables us to obtain the helical pitch of 12OF1M7 in the region shorter than about 30 smectic layers (≈100 nm). Strong absorption by organic molecules in the UV region places such a limit in measuring optical pitch of liquid crystal samples by a conventional selective reflection technique. Specifically, we have demonstrated that the pitch of about 16 layers just below the SmA-SmC^*_α transition can be obtained by acquiring DOR data from 21 freestanding films having consecutive layer thickness within a carefully chosen range of film thickness (41–61 layers).

Upon heating, the helical pitch shows a very steep drop through the SmC^*-SmC^*_α transition of 12OF1M7, levels off in the high temperature phase, and reaches a value of 16 layers just below the SmA^*-SmC^*_α transition. This limiting value of 16 layers for the helical pitch was obtained using

two methods: identifying the repetition of DOR data from 21 freestanding films having consecutive layer thicknesses and fitting DOR data from a 230-layer film using Berreman's 4 $\times 4$ matrix method. Within our experimental resolution, no jump in the helical pitch can be detected. Based on the fact that the symmetry does not change through this transition, the transition is equivalent to the well-known liquid-gas transition. Thus far both a jump in helical pitch as well as continuous evolution of helical pitch have both been reported for different compounds [37,39]. It would be extremely important to locate this intriguing critical point with a proper choice of binary mixtures and then investigate its critical behavior.

The analysis shows that the incommensurate nanoscale helical pitch (INHP) found in the SmC^*_α phase is due to the competition of the nearest-neighbor ferroelectric and the next-nearest-neighbor antiferroelectric interactions. By fitting to temperature variation of incommensurate nanoscale helical pitch data, we have obtained the ratio of the free energy expansion coefficients. Our results should inspire more theoretical work to get a better understanding of the molecular interactions of the relevant SmC^* variant phases.

ACKNOWLEDGMENTS

V.P.P. and J.K.V. thank Professor A. Fukuda and Dr. A. V. Emelyanenko for valuable discussions. V.P.P. was supported by the Irish Research Council for Science, Engineering and Technology (IRCSET). J.K.V. thanks the Science Foundation of Ireland for funding the facilities (Grant No. SFI 02-INI-I31). B.K.M., Z.Q.L., and C.C.H. are supported in part by the National Science Foundation, Solid State Chemistry Program, under Grant No. DMR-0106122.

[1] L. A. Beresnev, L. M. Blinov, V. A. Baikalov, E. P. Pozhidaev, G. V. Purvanetskas, and A. I. Pavluschenko, Mol. Cryst. Liq. Cryst. **89**, 327 (1982).
[2] A. D. L. Chandani, Y. Ouchi, H. Takezoe, A. Fukuda, K. Terashima, K. Furukawa, and A. Kishi, Jpn. J. Appl. Phys., Part 2 **28**, L1261 (1989).
[3] A. D. L. Chandani, E. Gorecka, Y. Ouchi, H. Takezoe, and A. Fukuda, Jpn. J. Appl. Phys., Part 2 **28**, L1265 (1989).
[4] N. Okabe, Y. Suzuki, I. Kawamura, T. Isozaki, H. Takezoe, and A. Fukuda, Jpn. J. Appl. Phys., Part 2 **31**, L793 (1992).
[5] T. Isozaki, T. Fujikawa, H. Takezoe, A. Fukuda, T. Hagiware, Y. Suzuki, and I. Kawamura, Jpn. J. Appl. Phys., Part 2 **31**, L1435 (1992).
[6] R. B. Meyer, L. Liebert, L. Strzelecki, and P. Keller, J. Phys. (France) Lett. **36**, L69 (1975).
[7] Y. Takanishi, K. Hiraoka, V. K. Agrawal, H. Takezoe, A. Fukuda, Jpn. J. Appl. Phys., Part 1 **30**, 2023 (1991).
[8] P. Mach, R. Pindak, A.-M. Levelut, P. Barois, H. T. Nguyen, C. C. Huang, and L. Furenlid, Phys. Rev. Lett. **81**, 1015 (1998).
[9] M. Fukui, H. Orihara, Y. Yamada, N. Yamamoto, and Y. Ishibashi, Jpn. J. Appl. Phys., Part 2 **28**, L849 (1989).
[10] N. M. Shtykov, A. D. L. Chandani, A. V. Emelyanenko, A. Fukuda, and J. K. Vij, Phys. Rev. E **71**, 021711 (2005).
[11] A. Fukuda, Y. Takanishi, T. Isozaki, K. Ishikawa, and H. Takezoe, J. Mater. Chem. **4**, 997 (1994), and references therein.
[12] D. A. Olson, X. F. Han, A. Cady, and C. C. Huang, Phys. Rev. E **66**, 021702 (2002).
[13] A. V. Emelyanenko and M. A. Osipov, Phys. Rev. E **68**, 051703 (2003).
[14] M. B. Hamaneh and P. L. Taylor, Phys. Rev. Lett. **93**, 167801 (2004).
[15] K. Hiraoka, Y. Takanishi, K. Skarp, H. Takezoe, and A. Fukuda, Jpn. J. Appl. Phys., Part 2 **30**, L1819 (1991).
[16] M. Cepic and B. Zeks, Mol. Cryst. Liq. Cryst. Sci. Technol., Sect. A **263**, 61 (1995).
[17] V. L. Lorman, Liq. Cryst. **20**, 267 (1996).
[18] V. Laux, N. Isaert, H. T. Nguyen, P. Cluzeau, and C. Destrade, Ferroelectrics **179**, 25 (1996).
[19] P. Mach, R. Pindak, A.-M. Levelut, P. Barois, H. T. Nguyen, H. Baltes, M. Hird, K. Toyne, A. Seed, J. W. Goodby, C. C. Huang, and L. Furenlid, Phys. Rev. E **60**, 6793 (1999).
[20] P. M. Johnson, S. Pankratz, P. Mach, H. T. Nguyen, and C. C. Huang, Phys. Rev. Lett. **83**, 4073 (1999).
[21] D. Schlauf, Ch. Bahr, and H. T. Nguyen, Phys. Rev. E **60**, 6816 (1999).
[22] H. Orihara, A. Fajar, and V. Bourny, Phys. Rev. E **65**, 040701(R) (2002).
[23] V. P. Panov, N. M. Shtykov, A. Fukuda, J. K. Vij, Y. Suzuki, R. A. Lewis, M. Hird, and J. W. Goodby, Phys. Rev. E **69**, 060701(R) (2004).
[24] V. P. Panov, Yu. P. Panarin, O. E. Panarina, J. K. Vij, and J. W. Goodby, in Tenth Conference on Ferroelectric Liquid Crystals, Stare Jablonki, Poland, 2005 (unpublished).
[25] N. M. Shtykov, J. K. Vij, and H. T. Nguyen, Phys. Rev. E **63**, 051708 (2001).
[26] N. M. Shtykov and J. K. Vij, Liq. Cryst. **28**, 1699 (2001).
[27] X. F. Han, D. A. Olson, A. Cady, J. W. Goodby, and C. C. Huang, Phys. Rev. E **65**, 010704(R) (2001).
[28] N. M. Shtykov, J. K. Vij, and V. P. Panov, J. Mater. Chem. **9**, 1383 (1999).
[29] V. P. Panov, J. K. Vij, A. Fukuda, J. W. Goodby, and H. T. Nguyen, in 20th International Liquid Crystal Conference, Ljubljana, Slovenia, 2004 (unpublished).
[30] D. A. Olson, X. F. Han, P. M. Johnson, A. Cady, and C. C. Huang, Liq. Cryst. **29**, 1521 (2002).
[31] B. K. McCoy, Z. Q. Liu, S. T. Wang, V. P. Panov, J. K. Vij, J. W. Goodby, and C. C. Huang, Phys. Rev. E **73**, 041704 (2006).
[32] S. Pankratz, P. M. Johnson, and C. C. Huang, Rev. Sci. Instrum. **71**, 3184 (2000).
[33] D. W. Berreman, J. Opt. Soc. Am. **62**, 502 (1972).
[34] A. Cady, X. F. Han, D. A. Olson, H. Orihara, and C. C. Huang, Phys. Rev. Lett. **91**, 125502 (2003).
[35] Yu. P. Panarin, V. P. Panov, O. E. Panarina, and J. K. Vij, in Tenth Conference on Ferroelectric Liquid Crystals, Stare Jablonki, Poland, 2005 (unpublished).

[36] P. M. Johnson, D. A. Olson, S. Pankratz, Ch. Bahr, J. W. Goodby, and C. C. Huang, Phys. Rev. E **62**, 8106 (2000).
[37] A. Cady, D. A. Olson, X. F. Han, H. T. Nguyen, and C. C. Huang, Phys. Rev. E **65**, 030701 (2002).
[38] C. C. Huang and J. M. Viner, Phys. Rev. A **25**, 3385 (1982).
[39] C. C. Huang, Z. Q. Liu, A. Cady, R. Pindak, W. Caliebe, P. Barois, H. T. Nguyen, K. Ema, K. Takekoshi, and H. Yao, Liq. Cryst. **31**, 127 (2004).